A Journal of the Gesellschaft Deutscher Chemiker

Angewandte International Edition GDCh Chemie

www.angewandte.org

Accepted Article

Title: Hyperbranched Vitrimer for Ultrahigh Energy Dissipation

Authors: Lin Cheng, Jun Zhao, Zhongqiang Xiong, Sijun Liu, Xuzhou Yan, and Wei Yu

To be cited as: *Angew. Chem. Int. Ed.* **2024**, e202406937

Link to VoR: https://doi.org/10.1002/anie.202406937

WILEY VCH

10.1002/anie.202406937

WILEY VCH

RESEARCH ARTICLE

Hyperbranched Vitrimer for Ultrahigh Energy Dissipation

Lin Cheng, Jun Zhao, Zhongqiang Xiong, Sijun Liu, Xuzhou Yan, Wei Yu*

Dr. L. Cheng, Dr. J. Zhao, Dr. Z. Xiong, Prof. S. Liu, Prof. X. Yan, Prof. W. Yu
Advanced Rheology Institute, School of Chemistry and Chemical Engineering, Frontiers Science Center for Transformative Molecules
Shanghai Jiao Tong University, Shanghai 200240, P. R. China
E-mail: wyu@sjtu.edu.cn

Supporting information for this article is given via a link at the end of the document.

Abstract: Polymers are ideally utilized as damping materials due to the high internal friction of molecular chains, enabling effective suppression of vibrations and noises in various fields. Current strategies rely on broadening the glass transition region or introducing additional relaxation components to enhance the energy dissipation capacity of polymeric damping materials. However, it remains a significant challenge to achieve high damping efficiency through structural control while maintaining dynamic characteristics. In this work, we propose a new strategy to develop hyperbranched vitrimers (HBVs) containing dense pendant chains and loose dynamic crosslinked networks. A novel yet weak dynamic transesterification between the carboxyl and boronic acid ester was confirmed and used to prepare HBVs based on poly (hexyl methacrylate-2-(4-ethenylphenyl)-5,5-dimethyl-1,3,2-dioxaborinane) P(HMA-*co*-ViCL) copolymers. The AB_n-type of macromonomers, the crosslinking points formed by the dynamic covalent connection via the associative exchange, and the weak yet dynamic exchange reaction are the three keys to developing high-performance HBV damping materials. We found that P(HMA-*co*-ViCL) 20k-40-60 HBV exhibited ultrahigh energy-dissipation performance over a broad frequency and temperature range, attributed to the synergistic effect of dense pendant chains and weak dynamic covalent crosslinks. This unique design concept will provide a general approach to developing advanced damping materials.

Introduction

Nowadays, vibrations and noises are ubiquitous in the industrial field, which can cause resonance, malfunctioning, or fatigue failure and threaten human health.[1] The relative frequency range of these vibration and noise sources predominantly falls between 0.01 and 300 Hz.[2] It is urgent to develop high-performance damping material over a wide frequency range to effectively suppress unwanted vibration and noise interference. Polymers are ideally suited as damping materials because of the high internal friction of chain relaxation, enabling effective dissipation of energy as heat during service.[3] Manipulating polymer viscoelasticity to enhance internal molecular frictions is the key to achieving high damping capacity ($tan\ \delta$ ≈ 0.3, which is defined by the ratio of loss modulus G'' and storage modulus G').[4] There are two major approaches to optimize the damping performance of polymers.[5] One direction is to shift and broaden the glass transition region with an apparent $tan\ \delta$ peak to the working temperature/frequency range by blending polymer,[6] copolymerization,[7] interpenetrating polymer networks,[8] and incorporating nanofillers.[9] However, materials at the glass transition region typically possess higher moduli in a relatively narrow temperature/ frequency range, which limits their applications in scenarios requiring soft, adaptable materials.[10] The other direction is introducing additional relaxation components such as pendant chains,[5,11] entanglements,[12] dynamic covalent bonds,[13] mechanical bonds,[14] hydrogen bonds,[15] coordination bonds[16] to endow highly damping capacity. Although these network defects or dynamic reversible bonds have already been reported to enhance the polymer damping performance effectively, challenges remain to maximize the utility of the additional relaxation components. To the best of our knowledge, none of the previous strategies can synergize damping, dynamic character, and pendant chains in one polymer.

It is well known that the critical state of sol-gel transition during the crosslinking of polymers exhibits power-law relaxation. The storage modulus G' and the loss modulus G'' depend on the frequency with the same power-law exponent, $G'{\sim}G''{\sim}\omega^n$.[17] As a result, the tangent loss becomes independent of frequency ($tan\ \delta{\sim}\omega^0$) over several decades of frequency. It implies that suitable design and control of the critical network would be an efficient approach to obtain desirable damping properties of polymeric materials. However, it remains a significant challenge to control the polymer network in the critical crosslinking state while possessing high damping capacity and dynamic characteristics. Achieving dynamic characteristics involves introducing dynamic covalent bonds,[13] yet there has been no report on accomplishing a critical crosslinking state while owning high energy dissipation performance for dynamic crosslinked polymers. The main reason might be that simply introducing dynamic covalent bonds makes it difficult to maintain the polymer network in a critical gel state.

10.1002/anie.202406937

RESEARCH ARTICLE

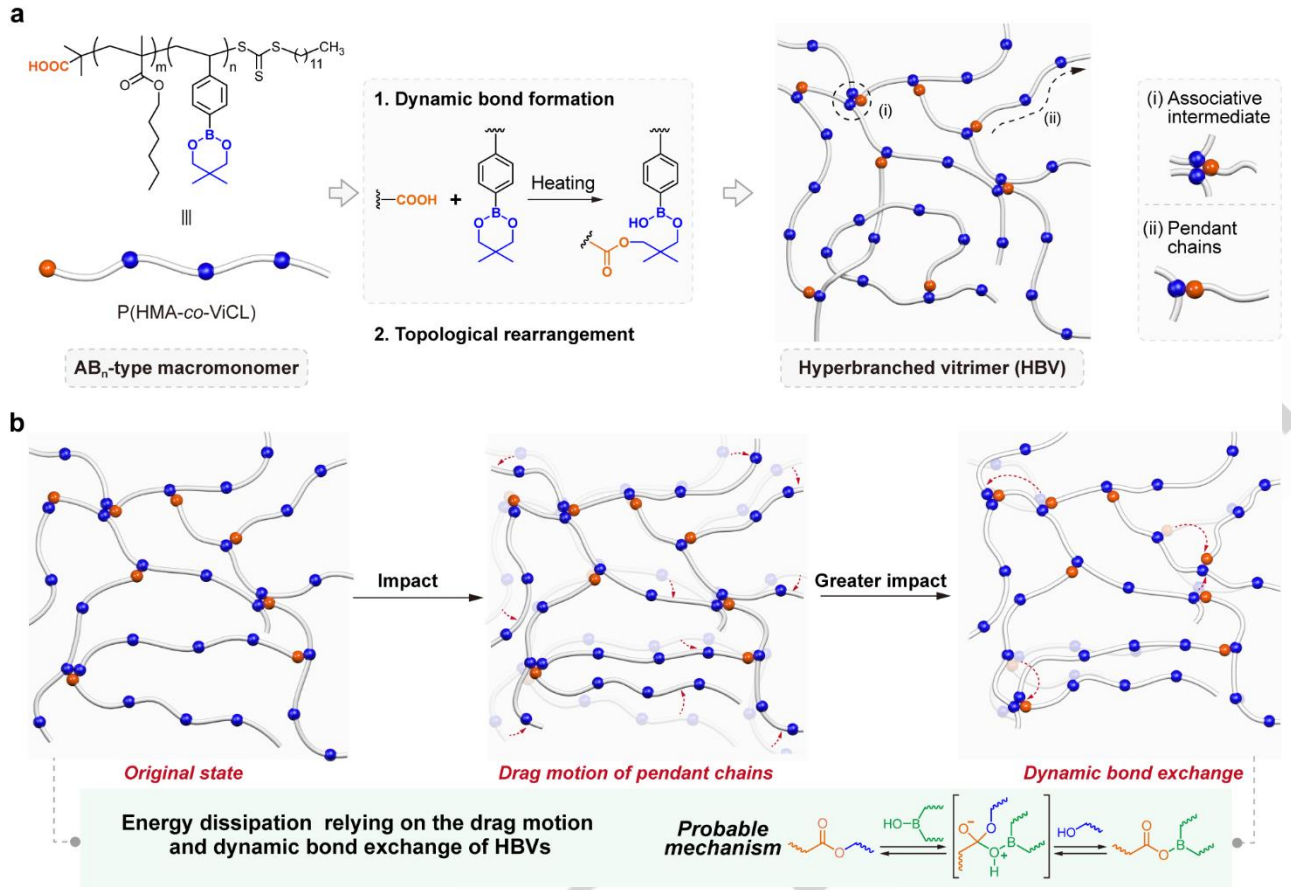

Figure 1. (a) Chemical structure and schematic representation of the hyperbranched vitrimer (HBV). (b) The possible energy-dissipation mechanism of HBV is the synergistic effect of the drag motion of dense pendant chains and dynamic bond exchange upon being subjected to external forces.

Inspired by the connection between rheology and associative exchange dynamic reaction in polymer networks,[18] we propose a new strategy to reach the critical state with a weak yet dynamic polymer precursor, which forms a weakly dynamic crosslinking network with hyperbranched topologies (hyperbranched vitrimer, HBV) and considerable amounts of pendant chains, as depicted in Figure 1a. The chain topology can be obtained and kept near the critical sol-gel transition by choosing a dynamic reversible reaction with a lower reaction equilibrium constant K_{eq}. The formation of this particular topology mainly depends on the dynamic reversible reaction character as well as the molecular structure factors of the precursor. However, the reported dynamic reversible reactions usually possess a relatively higher rate constant,[19] or a higher reaction equilibrium constant,[20] which leads to the formation of polymer networks with a low amount of defects. Therefore, finding a new dynamic reversible reaction with a low K_{eq} is the key to constructing dynamic polymer containing pendant chains.

Herein, we report a new strategy to develop hyperbranched vitrimers (HBVs) by regulating the structure of the polymer to be weakly crosslinked yet close to the critical state of sol-gel transition through the dynamic reversible reaction character (Figure 1a). In detail, the associative intermediates serve as the dynamic crosslinking points and one main energy-dissipation motif, resulting in the formation of loose dynamic crosslinked networks. The dense pendant chains are formed by a dynamic associative exchange reaction between the unique AB_n-type of macromonomers with a relatively high molecular weight and comonomer content. Near critical gel state maximizes the density of network defects. Under the synergistic effect of the drag motion of pendant chains and dynamic bond exchange when subjected to external forces (Figure 1b), the obtained P(HMA-*co*-ViCL) 20k-40-60 HBV exhibits excellent energy-dissipation and damping capacity over a broad frequency and temperature range. We hope the present study may motivate the further development of high-performance damping materials.

10.1002/anie.202406937

RESEARCH ARTICLE

Results and Discussion

Model reaction. A relatively weak yet dynamic reversible reaction is the key to constructing HBV. Different from the reported dynamic covalent bonds with a large equilibrium constant or high reaction rate,[19-20] we explore a special transesterification reaction between carboxyl and boronic acid ester. Propanoic acid (PA) and boric acid triethyl ester (BATEE) were chosen as model small molecules to confirm the possibility of transesterification. PA and BATEE were mixed in 3:1 stoichiometric ratio at 90 °C for 168 h (Figure 2a). Figure 2b (i, ii, iii) and Figure S1 showed the ^{1}H NMR analysis of the forward reaction. We found the appearance of signals at 4.08-4.14 ppm (q, 2H, -O-C$\boldsymbol{H}_2$-), 2.24-2.32 ppm (q, 2H, -C$\boldsymbol{H}_2$-), 1.14-1.22 ppm (t, 3H, -C$\boldsymbol{H}_3$), 0.98-1.06 ppm (m, 3H, -C$\boldsymbol{H}_3$), which correspond to the target product of ethyl propanoate (EP). Likewise, EP and BA were chosen as reactants, which could generate PA and BATEE under the same conditions, as shown in Figure 2b (iv) and Figure S2. These results confirm the reversibility of the reaction between carboxyl and boronic acid ester. The conversion yield of the model reaction was also calculated from ^{1}H NMR spectra (Figure S3). The conversion yields of the forward reaction and backward reaction after 168 h were close to 44% and 36%, respectively. However, the model reaction was very slow in the first 40 h, where both conversion yields were below 10%. In another aspect, it indicates that the transesterification between carboxyl and boronic acid ester is rather slow and weak, as compared to the typical dynamic reversible covalent reactions like dioxaborolane metathesis.[21]

Design, synthesis, and structure characterization of P(HMA-*co*-ViCL) HBVs. Besides the weak yet dynamic reversible bond, it is also necessary to design the appropriate precursors containing the desired functional groups with proper proportions to prepare an HBV. In this study, we synthesized a series of P(HMA-*co*-ViCL) copolymers terminated by single-ended carboxyl through the reversible addition−fragmentation chain transfer (RAFT) reaction, with carboxyl-terminated trithiocarbonates utilized as the RAFT agent, azodiisobutyronitrile (AIBN) as the initiator, HMA and ViCL as the comonomers (Figure 3a). Meanwhile, two control copolymers, i.e., poly(hexyl methacrylate-styrene), named P(HMA-*co*-St), and poly(hexyl methacrylate-2-(4-ethenylphenyl)-5,5-dimethyl-1,3,2-dioxaborinane) terminated with phenyl group, named P(HMA-*co*-ViCL)-CDB, were prepared for comparison, in which the former features only contained the terminal carboxyl but without boronic acid ester, the later one only owned the boronic acid ester but without terminal carboxyl (Figure 3b). The synthetic procedures of all monomers and copolymers were summarized in the Supporting Information. The actual molecular structure parameters of copolymers are listed in Table 1. The molecular weight of copolymers mainly includes two series, i.e., 5 kg/mol and 20 kg/mol (5k and 20k for short), which could be well regulated by the usage amount of RAFT agent and AIBN. The molar ratio of boronic acid ester is about 10% to 60%.

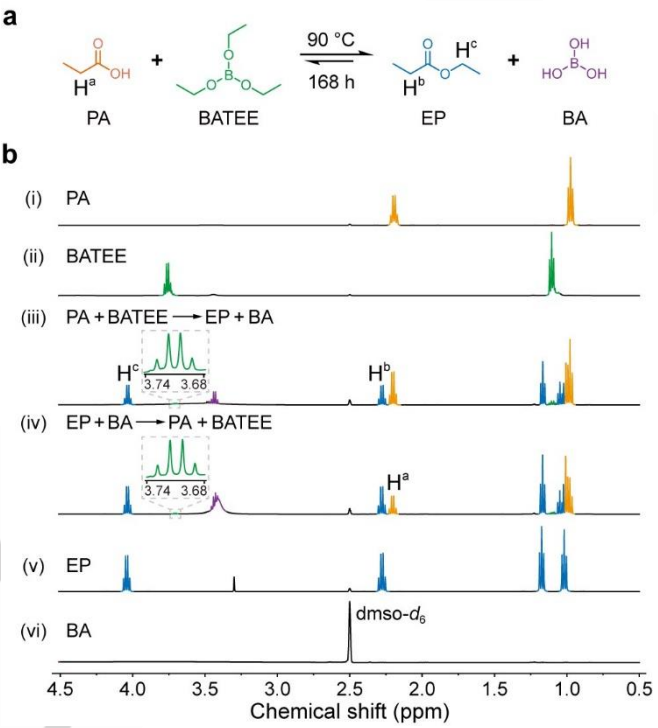

Figure 2. (a) Transesterification model reaction between PA and BATEE at 90 °C for 168 h. (b) ^{1}H NMR spectra of transesterification reaction mixtures at 90 °C for 168 h in DMSO.

In the previous section, we have demonstrated that carboxyl and boronic acid ester could react according to the model reaction between PA and BATEE. P(HMA-*co*-ViCL) copolymers are AB_n-type of macromonomers, which form hyperbranched polymers with the reaction between carboxyl at the end of molecular chains and boronic acid ester dangling in the molecular chains. One possibility of network formation is through the mechanically interlocked loops, and the other is through the associative intermediates (Figure 1a). It has been illustrated that the associative intermediates can act as effective crosslinking points.[18] Whether the P(HMA-*co*-ViCL) copolymers could generate hyperbranched dynamic networks with considerable amounts of pendent chains is closely related to the molecular weight and ViCL molar ratio of copolymers.

In addition, the thermal analysis of P(HMA-*co*-HMA) and control copolymers were studied by DSC, as shown in Figure S8 and Table 1. All the synthesized copolymers have just one glass transition temperature (T_g), which increases with the increasing

10.1002/anie.202406937

RESEARCH ARTICLE

molecular weight of copolymers and the molar ratio of ViCL comonomers. Notably, the T_g P(HMA-*co*-St) without boronic acid ester is reduced as compared with copolymers having the same molecular weight and monomer molar ratio. It also suggests that the dangling boronic acid ester in molecular chains plays a crucial role in the topology construction and performance regulation of copolymers.

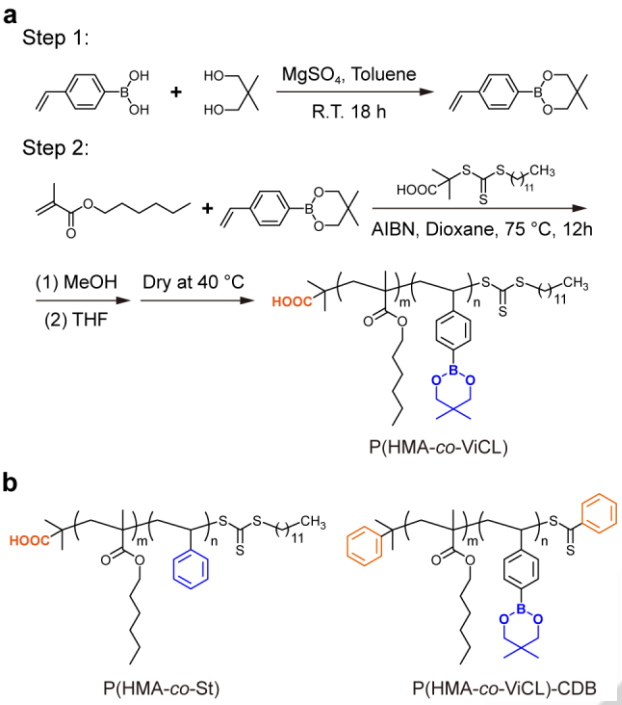

Figure 3. (a) The synthetic routes of P(HMA-*co*-ViCL) copolymers terminated by a single-ended carboxyl group. (b) Chemical structures of two control copolymers.

Table 1. Molecular structure parameters of P(HMA-*co*-ViCL) and control copolymers.

Sample name	n%[a] (HMA)	n%[a] (ViCL)	M_n[b] (kg/mol)	PDI[b]	T_g[c] (°C)
P(HMA-*co*-ViCL) 5k-90-10	91	9	7.2	1.69	-26
P(HMA-*co*-ViCL) 5k-80-20	81	19	7.0	1.54	-18
P(HMA-*co*-ViCL) 5k-40-60	38	62	5.5	1.30	22
P(HMA-*co*-ViCL) 20k-90-10	90	10	22.9	1.61	-12
P(HMA-*co*-ViCL) 20k-80-20	78	22	26.9	1.73	20
P(HMA-*co*-ViCL) 20k-40-60	40	60	14.7	1.20	28
P(HMA-*co*-St) 20k-80-20	79	21	15.4	1.23	-10
P(HMA-*co*-ViCL) 20k-80-20-CDB	78	22	15.8	1.19	12

[a] n% (molar ratio of comonomer) is calculated from ^{1}H NMR spectra. [b] M_n and PDI are obtained from GPC test. [c] T_g is obtained from the DSC test.

Linear viscoelasticity of P(HMA-*co*-ViCL) HBVs. Rheology is a convenient and effective method to reveal the topology and dynamic characteristics of a polymer. We utilized the time-temperature superposition (TTS) principle to construct the master curves for a comprehensive demonstration of linear viscoelasticity over a wide range of frequencies. Here, it's worth noting that the master curves were superposed of the polymer chain segmental motions on the premise of compliance with the TTS principle.[4] Firstly, we investigated the effect of monomer type and the capping group on the linear viscoelasticity of copolymers. Fixed the molecular weight as 20 kg/mol, the molar ratio of HMA as 80%, three kinds of copolymers with different functional groups were designed, including P(HMA-*co*-ViCL) 20k-80-20, P(HMA-*co*-St) 20k-80-20, and P(HMA-*co*-ViCL) 20k-80-20-CDB. Because of the different T_g values of P(HMA-*co*-ViCL) and control copolymers, we compared their linear viscoelasticity in the iso-frictional condition at the reference temperature of T_{ref}=T_g+40 °C. The rheological master curves of storage modulus (G'), loss modulus (G'') and loss factor ($tan\ \delta$) are presented in Figure 4a-c. The evident failure of TTS above 70 °C was found for P(HMA-*co*-ViCL) 20k-80-20. This result has also provided important evidence for the reversibility of model reaction between carboxyl and boronic acid ester, while at the same time showing obvious dynamic behaviors of P(HMA-*co*-ViCL) 20k-80-20. The master curve of P(HMA-*co*-ViCL) 20k-80-20 was established by superposing the high-frequency part of moduli at higher temperatures. That is, the master curves were built under the guidance of high-ω G'' data, where the shift factors $a_{T,high}$ reflected the temperature dependence of the modulus contributed by the Rouse-type motion.[18] The variation of the horizontal shift factor ($a_{T,high}$) of three copolymers fit the Williams-Landel-Ferry (WLF) equation well (Figure S9). We found no terminal relaxation but a gradual trend to show a plateau at the lowest frequency for P(HMA-*co*-ViCL) 20k-80-20. Meanwhile, G' and G'' are very close to each other over a wide range of frequencies, as also illustrated in the weak dependence of $tan\ \delta$ on frequency (Figure 4c). This is the characteristic of critical gel according to the Winter-Chambon criterion.[17] In contrast, the master curves of P(HMA-*co*-St) 20k-80-20 and P(HMA-*co*-ViCL) 20k-80-20-CDB

10.1002/anie.202406937

conformed well with the TTS principle. The direct comparison between the three copolymers in Figure 4a-c shows that each of the three copolymers exhibited indistinguishable behavior in the glassy-to-rubbery transition zone. This regime is associated with localized relaxations on the length scale of the monomeric segments. An apparent deviation begins when $a_T\omega < 10$ rad/s, the two control copolymers manifested the liquid-like terminal relaxation ($G'\sim\omega^2$ and $G''\sim\omega$). Because the critical entanglement molecular weight (M_e) is 19000 g/mol for polystyrene PS and 33100 g/mol for poly (hexyl methacrylate) PHMA,[22] the terminal relaxation of two control polymers corresponds to the Rouse relaxation of the unentangled chains. However, P(HMA-*co*-ViCL) 20k-80-20 requires more than five additional orders of time scales to achieve ultimate terminal flow. The essential reason for this difference is attributed to the different molecular structures of the three copolymers. For P(HMA-*co*-ViCL) 20k-80-20, the carboxyl at the end of molecular chains would react with boronic acid ester in the molecular chains, resulting in hyperbranched topologies that are close to the critical gel. The hyperbranched molecules are further crosslinked by the associative intermediates and interlocked loops. The formed networks have a low crosslinking density and are abundant in pendant chains. Therefore, the choice of the comonomer and RAFT agent is the key to constructing HBVs.

Besides the feasibility and reversibility of novel transesterification between carboxyl and boronic acid ester, other influences on the HBVs are the structure factors of copolymers, including molecular weight and molar ratio of comonomer. With the fixed number molecular weight as 5 kg/mol and 20 kg/mol, six kinds of P(HMA-*co*-ViCL) copolymers with different molecular weights and monomer molar ratios were obtained by regulating the ViCL content as 10%, 20%, and 60%, respectively. The dynamic moduli of P(HMA-*co*-ViCL) copolymers were measured, and master curves were constructed under the guidance of high-ω G'' data according to the TTS principle, as shown in Figure 4d-f and Figure S10a. The horizontal shift factors are plotted in Figure S11, which fit the Williams-Landel-Ferry (WLF) equation well. For the three P(HMA-*co*-ViCL) copolymers with M_n ≈5 kg/mol, their master curves demonstrate a predominantly viscous response to the imposed deformation, as G' remains smaller than G'' at nearly all frequencies. Failure of TTS is very weak and can be ignored. The 5k series P(HMA-*co*-ViCL) copolymers exhibit pronounced Rouse-like relaxation character, with the scaling relations of the terminal region ($G'\sim\omega^2$ and $G''\sim\omega$). The stress of the three copolymers could relax completely within a short time scale (Figure S12a-c), aligning with the results obtained from the rheological master curves. Nonetheless, we found a close terminal relaxation time of P(HMA-*co*-ViCL) 5k-80-20 and P(HMA-*co*-St) 20k-80-20, as presented in Figure S13. It is ascribed to larger branched molecules formed in P(HMA-*co*-ViCL) 5k-80-20 due to the dynamic reaction between the carboxyl at chain ends and boronic acid ester. However, there is no sufficient evidence of network formation in 5k series of polymers, probably due to the synergic effect of weak dynamic reaction and short length of chains.

When the molecular weight was increased to about 20 kg/mol, the storage modulus G', loss modulus G'', and loss factor $tan\,\delta$ for P(HMA-*co*-ViCL) copolymers overlap with those 5k samples in the high-frequency region at $a_T\omega \geq 10$ rad/s, consistent with the no influence of chain length on the short time scale dynamics such as segmental relaxation. However, the comonomer content strongly affects the long-timescale relaxation behavior when the molecular weight is large enough. Specifically, for P(HMA-*co*-ViCL) 20k-90-10, manifested a Rouse-like relaxation process analogous to 5k series copolymers, but it takes more than two orders of time scale to achieve terminal relaxation. This observation was further confirmed by the stress relaxation curves of P(HMA-*co*-ViCL) 20k-90-10, where the stress could relax completely (Figure S12d). For other 20k series P(HMA-*co*-ViCL) copolymers, with ViCL monomer content from 15% to 60%, obvious failures of TTS were observed when the temperature was above 70 °C (Figure 4d-f and Figure S14), thereby implying the simultaneous existence of two relaxation behaviors with different temperature dependences, namely the dynamic reaction and chain relaxation. The terminal relaxation time of 20k series polymers increases with the ViCL content, showing a transition at around 20%. This transition happens when a plateau appears in the storage modulus, denoting the dynamic crosslinking of hyperbranched polymers. As the ViCL content increased to 60%, the plateau moduli of P(HMA-*co*-ViCL) copolymers was increased to about ~20 kPa (Figures S14-S16), which was close to the same order of plateau moduli for bottlebrush melts and networks.[23] Simultaneously, the stress of P(HMA-*co*-ViCL) 20k-40-60 could achieve relaxation while maintaining a plateau over a longer time scale, which is a characteristic feature of vitrimers (Figure S12f). Furthermore, we estimated the equilibrium crosslinking density by the cyclic frequency sweep rheological methods, as demonstrated in Figures S15 and S16. The average molecular weight between crosslinks (i.e. associative intermediates), M_x, could be estimated according to $M_x = \rho RT/G_N$, as summarized in Table S1. The average molecular weight between crosslinks M_x is increased with the increase in temperature, that is, the crosslinking density of HBV is decreased with temperature. This is primarily because the dissociation reaction is more prone to

occurring at higher temperatures. These findings further validated the formation of the hyperbranched vitrimer topologies. But compared to the complicated synthetic routes of bottlebrush polymers, the one-step polymerization strategy in our work is simpler and more convenient to construct supersoft elastomers. Moreover, from the comparison of master curves, it also reflects in the time-scale separation between different relaxation modes, i.e., glass, pendant short chains, crosslinked plateau, and the terminal relaxation processes. Especially for P(HMA-*co*-ViCL) 20k-40-60, it requires more than 11 orders of magnitude time scales to complete the relaxation process of the overall polymer topology. Therefore, the molecular weight and ViCL content are the major molecular structure factors to construct dynamic polymers containing pendant chains. It is worth noting that the loss factor ($tan\ \delta$) of P(HMA-*co*-ViCL) 20k-40-60 is above 0.3 over a broad frequency range of nearly 10 orders of magnitude (Figure 4f and Figure S10a), which presents excellent energy-dissipation property. In addition, the temperature dependence P(HMA-*co*-ViCL) 20k-40-60 HBV was also assessed by cyclic temperature ramp tests. As demonstrated in Figure S17, both G' and G'' dropped by nearly two orders of magnitude when the temperature was ramped up from 80 to 170 °C. The opposite process in which the temperature was ramped down led to the opposite viscoelastic transition. The ramp curves roughly overlapped with each other, indicative of a relatively good thermoreversible performance. Importantly, the loss factor $tan\ \delta$ was greater than 0.3 within the tested temperature range, indicating the remarkable damping capacity of P(HMA-*co*-ViCL) 20k-40-60 HBV over a wide temperature range. Thus, P(HMA-*co*-ViCL) 20k-40-60 can be utilized as an excellent damping material, whose energy dissipation mechanism is also directly associated with the multiscale dynamic mechanical relaxation character.

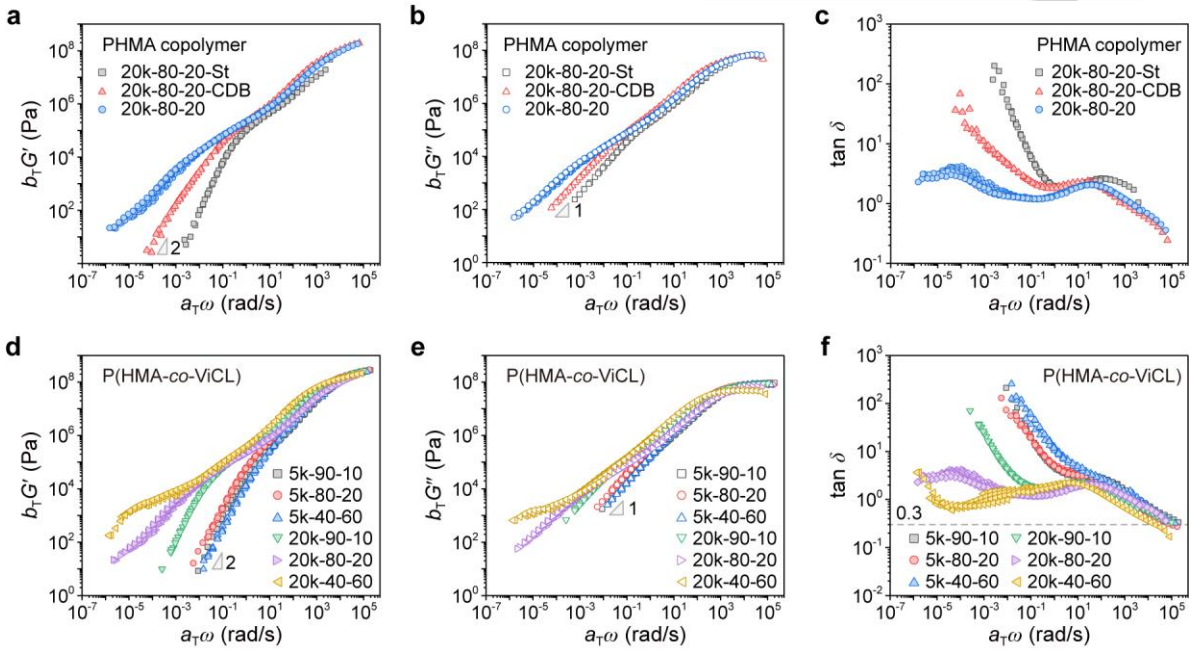

Figure 4. (a) Frequency dependence of storage modulus G', (b) loss modulus G'' and (c) loss factor $tan\ \delta$ for three copolymers with different functional groups. (d) Storage modulus G', (e) loss modulus G'' and (f) loss factor $tan\ \delta$ master curves of six P(HMA-*co*-ViCL) copolymers with different molecular weights and monomer molar ratios. The master curves are superposed of the polymer chain segmental motions in accordance with the TTS principle at the reference temperature of T_{ref}=T_g+40 °C.

The energy-dissipation property of P(HMA-*co*-ViCL) HBVs. We first compared the energy-dissipation properties of P(HMA-*co*-ViCL) copolymers with commercial damping materials and linear polymers by the falling ball tests. As shown in Figure 5a-b, P(HMA-*co*-ViCL) copolymers owned lower load force, especially for P(HMA-*co*-ViCL) 20k-40-60 HBV, the peak of its load force was ~7 times less than those of the control commercial damping materials. Moreover, P(HMA-*co*-ViCL) 20k-40-60 HBV could reduce the impact force up to 90% within 0.6 s (Figures S18 and S19), indicating excellent energy-dissipation performance. Then, we carried out compressive stress-strain tests to further characterize the energy-dissipation property of P(HMA-*co*-ViCL) 20k-40-60 HBV (Figure 5c). From four loading/unloading cycles (at a fixed level of 60%), P(HMA-*co*-ViCL) 20k-40-60 HBV showed a significantly raised hysteresis area along with the increase of the compression rate. The dissipated energy of HBVs increased from 0.26 MJ/mol at 0.05 s^{-1} to 1.20 MJ/mol at 2.08 s^{-1}, exhibiting compression rate-dependent mechanical behaviors. Moreover, the damping capacity of P(HMA-*co*-ViCL) 20k-40-60 HBV has exceeded 75%, showcasing excellent energy-dissipation

10.1002/anie.202406937

performance. These results imply that P(HMA-*co*-ViCL) 20k-40-60 is sensitive to the strain rate and can dissipate energy effectively during the impact process.

To get a deeper insight into the energy-dissipation property of P(HMA-*co*-ViCL) copolymers, a strain-rate frequency superposition (SRFS) approach was adopted to discern the effects of strain rate on the time scale of a structural relaxation process via a rheometer.[24] Specifically, we carried out a series of frequency-dependent rheological measurements at a constant strain-rate amplitude ($\dot{\gamma}$) ranging from 0.01 to 5.0 s^{-1}, as shown in Figure S20. Under a fixed strain-rate amplitude, a dynamic oscillatory frequency sweep was performed from high frequency to low frequency, and the corresponding strain amplitude increased linearly, equivalent to an increasing force or impact on the material. Accordingly, the frequency sweep curves at different $\dot{\gamma}$ can be obtained for four P(HMA-*co*-ViCL) copolymers with different molecular weights and monomer molar ratios (Figure S21). Based on these experimental results, we can differentiate the contribution from the stored elastic work (W_e) and viscous dissipated energy (W_s) under applied deformation according to Eq. 1[24]:

$$W = \int_0^{\gamma_0} \sigma d\gamma \approx \frac{1}{2} G_1'(\gamma_0, \omega)\gamma_0^2 + \frac{\pi}{4} G_1''(\gamma_0, \omega)\gamma_0^2 \quad (1)$$

where W is the total work, σ is the shear stress, γ is the shear strain, γ_0 is the experimental strain amplitude, ω is the angular frequency, G_1' and G_1'' are the fundamental in-phase and out-of-phase harmonic moduli. Here, we mainly consider the moduli values of the fundamental frequency (n=1) to perform calculations. The first term on the right side of Eq. 1 denotes the stored elastic work (W_e), and the second term denotes the viscous dissipated energy (W_s).

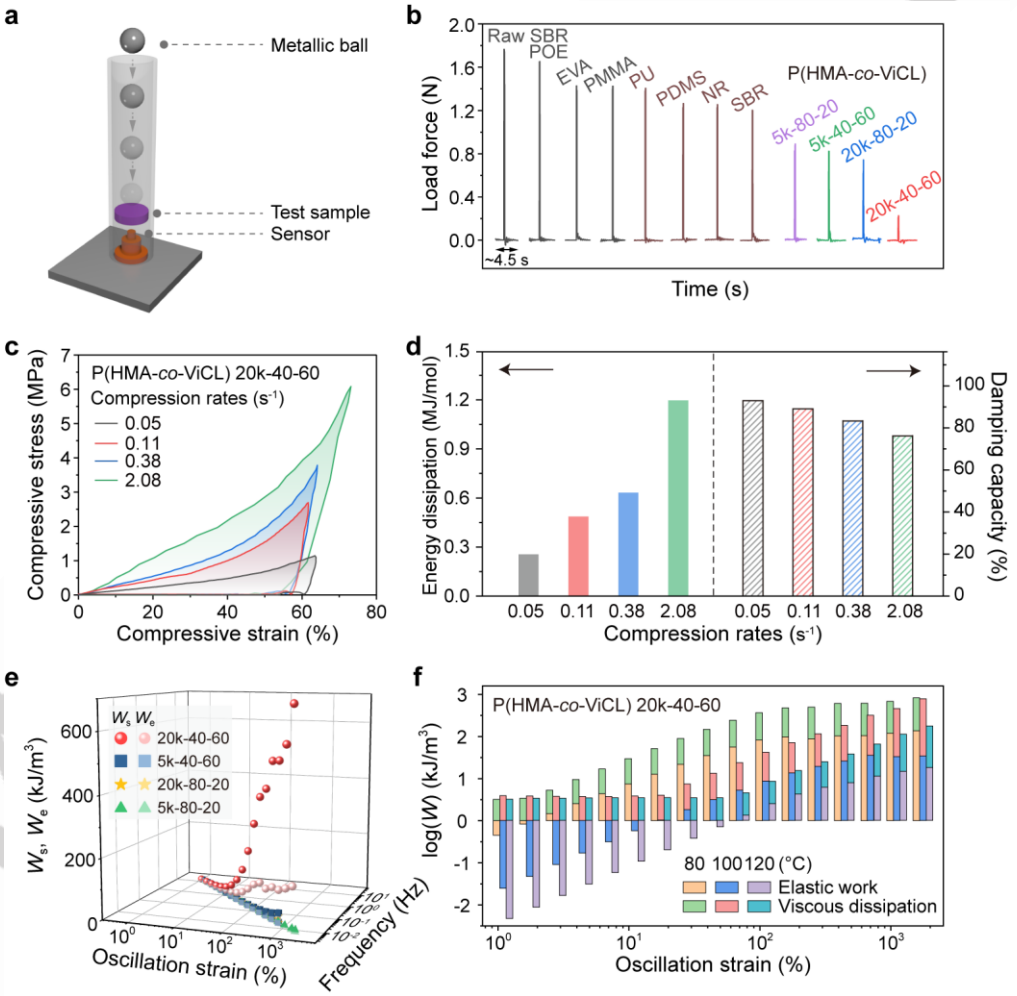

Figure 5. Comparison of energy-dissipation properties of P(HMA-*co*-ViCL) copolymers and other commercial damping materials. (a) Scheme of the falling ball test on selected damping materials. (b) The load force of different damping materials obtained from the falling ball tests at 80 °C. (c) The compressive stress-strain curves of P(HMA-*co*-ViCL) 20k-40-60 with different compression rates at 80 °C. (d) Energy dissipation and damping capacity of P(HMA-*co*-ViCL) 20k-40-60 calculated from their cyclic compressive curves. (e) 3D scatter plots of the viscous dissipated energy (W_s) and stored elastic work (W_e) as a function of strain amplitude (γ_0) and frequency for four P(HMA-*co*-ViCL) copolymers with different molecular weights and monomer molar ratios at 80 °C ($\dot{\gamma}$= 1.0 s^{-1}). (f) The total work of P(HMA-*co*-ViCL) 20k-40-60 ($\dot{\gamma}$= 1.0 s^{-1}) at 80 °C, 100 °C, 120 °C, respectively.

10.1002/anie.202406937

The viscoelasticity is the significant feature of deformation properties for polymer, which is more closely associated with its own topology and molecule structure. SRFS approach is a good combination to investigate energy dissipation with viscoelasticity for damping materials. The calculated viscous dissipated energy (W_s) and stored elastic work (W_e) of Eq. 1 were depicted in Figure 5e and Figures S22 and S23, respectively. We observed that the viscous dissipated energy contributed to the most input energy for four P(HMA-*co*-ViCL) copolymers. All the samples dissipated similar energy under small oscillatory strains, but the dissipated energy of P(HMA-*co*-ViCL) 20k-40-60 HBV quickly exceeded those of the other three copolymers as the oscillatory strain increased. For instance, at a strain amplitude of 1000% and strain rate of 1.0 s^{-1}, the viscous dissipated energy of P(HMA-*co*-ViCL) 20k-40-60 HBV is about 176 times that of P(HMA-*co*-ViCL) 5k-80-20. Meanwhile, the total work of each copolymer increased with the strain rate increasing from 0.01 to 5.0 s^{-1} (Figure S22). The outstanding energy-dissipation property of P(HMA-*co*-ViCL) 20k-40-60 could be attributed to the particular hyperbranched dynamic network. The energy-dissipation is mainly accomplished by the repeating drag motion of pendant chains under the imposed stress. Moreover, the reversible destruction and reconstruction of dynamic covalent bonds in P(HMA-*co*-ViCL) 20k-40-60 HBV also provide a potential mechanism for energy dissipation, where the external mechanical energy can be converted into thermal energy (Figure 1b). The synergistic effect of these aspects endows an excellent energy-dissipation property for P(HMA-*co*-ViCL) 20k-40-60 HBV.

Furthermore, we investigated the influence of temperature on the energy-dissipation behavior of P(HMA-*co*-ViCL) 20k-40-60 HBV. The dynamic oscillatory frequency sweep was carried out via SRFS approach at 80 °C, 100 °C, 120 °C, respectively (Figures S24 and S25). The storage moduli (G') were all greater than the loss moduli (G'') of P(HMA-*co*-ViCL) 20k-40-60 HBV at the three temperatures, G' and G'' dropped faster in the low-frequency region with an increase in the strain rate. The corresponding viscous dissipated energy (W_s) and stored elastic work (W_e) were also calculated by Eq. 1, as shown in Figure 5f and Figure S26. It can be found that energy dissipation is mainly dominated by viscous dissipation. Despite a slight drop of viscous dissipated energy as the temperature rises, P(HMA-*co*-ViCL) 20k-40-60 HBV still possesses an excellent energy-dissipation property at a higher temperature than those of other copolymers.

Conclusion

In summary, we have presented a new strategy in which dynamic reaction character is utilized to regulate the structure and mechanical properties of polymer networks. The hyperbranched dynamic polymer networks containing dense pendant chains could be prepared by choosing a weak yet dynamic reversible bond. The feasibility and reversibility of a novel transesterification reaction between carboxyl and boronic acid ester were proved by ^{1}H NMR and rheological results. Hyperbranched vitrimers were obtained from AB_n-type of P(HMA-*co*-ViCL) macromonomers containing end-capped carboxyl and pendant boronic acid ester, which could be easily prepared by one-step polymerization. The linear viscoelasticity revealed the dynamic reversibility of the reaction, and the transition to power-law relaxation. It is found that P(HMA-*co*-ViCL) 20k-40-60 HBV exhibited ultrahigh energy-dissipation performance (loss factor larger than 0.3) over a broad frequency and temperature range, which exceeded typical state-of-the-art damping materials. The energy-dissipation mechanism is due to the synergistic effect of the drag motion of pendant chains and dynamic bond exchange. The successful synthesis and uniqueness of P(HMA-*co*-VICL) HBVs provide a new route for the design and preparation of novel damping materials.

Acknowledgements

W.Y. acknowledges the financial support from the National Natural Science Foundation of China (Nos. 52333001, 51625303). L.C. acknowledges the financial support from the National Natural Science Foundation of China (Nos. 22303050) and the China Postdoctoral Science Foundation (2022M722069).

Keywords: Hyperbranched Vitrimer • Transesterification • Pendant Chain • Linear Viscoelasticity• Energy Dissipation

[1] a) R. S. Lakes, T. Lee, A. Bersie, Y. Wang, *Nature* **2001**, *410*, 565–567; b) M. S. Qatu, M. K. Abdelhamid, J. Pang, G. Sheng, *Int. J. Veh. Noise Vib.* **2009**, *5*, 1–35.

[2] a) Z. Wang, J. Wang, J. Ayarza, T. Steeves, Z. Hu, S. Manna, A. P. Esser-Kahn, *Nat. Mater.* **2021**, *20*, 869−874. b) J. Chu, G. Zhou, X. Liang, H. Liang, Z. Yang, T. Chen, *Mater. Today Commun.* **2023**, *36*, 106464.

[3] a) T. Sun, T. Kurokawa, S. Kuroda, A. B. Ihsan, T. Akasaki, K. Sato, M. A. Haque, T. Nakajima, J. Gong, *Nat. Mater.* **2013**, *12*, 932–937; b) D. Ratna, B. C. Chakraborty, *Polymers for vibration damping applications*, Elsevier, Amsterdam, Netherlands, **2020**; c) A. A. Gusev, K. Feldman, O. Guseva, *Macromolecules* **2010**, *43*, 2638–2641; d) Y. Wu, Y. Wang, X. Guan, H. Zhang, R. Gao, C. Cui, D. Wu, Y. Cheng, Z. Ge, Z. Zheng, Y. Zhang, *Adv. Mater.* **2023**, *35*, 2306882.

[4] a) J. D. Ferry, *Viscoelastic properties of polymers*, 3rd ed., New York, **1980**; b) C. M. Roland, *Viscoelastic behavior of rubbery materials*, Oxford University Press, **2011**.

[5] a) H. Yamazaki, M. Takeda, Y. Kohno, H. Ando, K. Urayama, T. Takigawa, *Macromolecules* **2011**, *44*, 8829–8834.

[6] a) Y. Li, Q. Lian, Z. Lin, J. Cheng, J. Zhang, *J. Mater. Chem. A* **2017**, *5*, 17549–17562; b) W. Wang, D. Zhao, J. Yang, T. Nishi, K. Ito, X. Zhao, L. Zhang, *Sci. Rep.* **2016**, *6*, 22810; c) X. Zhao, K. Niu, Y. Xu, Z. Peng, L. Jia, D. Hui, L. Zhang, *Compos.: Part B* **2016**, *107*, 106–112.

[7] a) F. Faghihi, N. Mohammadi, P. Hazendonk, *Macromolecules* **2011**, *44*, 2154–2160; b) J. Kim, M. M. Mok, R. W. Sandoval, D. J. Woo, J. M. Torkelson, *Macromolecules* **2006**, *39*, 6152–6160.

[8] a) D. Klempner, *Angew. Chem. Int. Ed.* **1978**, *17*, 97–106; b) E. Croisier, S. Liang, T. Schweizer, S. Balog, M. Mionic, R. Snellings, J. Cugnoni, V. Michaud, H. Frauenrath, *Nat. Commun.* **2014**, *5*, 4728; c) X. Lv, Z. Huang, C. Huang, M. Shi, G. Gao, Q. Gao, *Compos.: Part B* **2016**, *88*, 139–149.

[9] a) A. Joy, S. Varughese, S. Shanmugam, P. Haridoss, *ACS Appl. Nano Mater.* **2019**, *2*, 736–743; b) S. Ganesh, S. N. Subraveti, S. R. Raghavan, *ACS Appl. Mater. Interfaces* **2022**, *14*, 20014–20022; c) J. Suhr, N. Koratkar, P. Keblinski, P. Ajayan, *Nat. Mater.* **2005**, *4*, 134–137; d) J. Yin, H. Xiao, P. Xu, J. Yang, Z. Fan, Y. Ke, X. Ouyang, G. Liu, T. Sun, S. Cheng, P. Yin, *Angew. Chem. Int. Ed.* **2021**, *60*, 22212 –22218; e) J. Feng, B. Safaei, Z. Qin, F. Chu, *Compos. Sci. Technol.* **2023**, *233*, 109925.

[10] H. Xiang, X. Li, B. Wu, S. Sun, P. Wu, *Adv. Mater.* **2023**, *35*, 2209581.

[11] a) L. Xia, C. Li, X. Zhang, J. Wang, H. Wu, S. Guo, *Polymer* **2018**, *141*, 70–78; b) K. Urayama, T. Miki, T. Takigawa, A. Kohjiya, *Chem. Mater.* **2004**, *16*, 173–178.

[12] a) S. E. Neumann, J. Kwon, C. Gropp, L. Ma, R. Giovine, T. Ma, N. Hanikel, K. Wang, T. Chen, S. Jagani, R. O. Ritchie, T. Xu, O. M. Yaghi, *Science* **2024**, *383*, 1337–1343; b) J. Huang, Y. Xu, S. Qi, J. Zhou, W. Shi, T. Zhao, M. Liu, *Nat. Commun.* **2021**, *12*, 3610; c) W. Shi, T. Zhou, B. He, J. Huang, M. Liu, *Angew. Chem. Int. Ed.* **2024**, e202401845.

[13] a) J. Lee, B. B. Jing, L. E. Porath, N. R. Sottos, C. M. Evans, *Macromolecules* **2020**, *53*, 4741–4747; b) X, Zeng, X. Zeng, J. Fan, J. Li, Z. Wang, R. Sun, L. Ren, X. Xia, *ACS Mater. Lett.* **2022**, *4*, 874–881; c) J. Luo, X. Zhao, H. Ju, X. Chen, S. Zhao, Z. Demchuk, B. Li, V. Bocharova, J. Y. Carrillo, J. K. Keum, S. Xu, A. P. Sokolov, J. Chen, P. Cao, *Angew. Chem. Int. Ed.* **2023**, e202310989.

[14] a) X. Yang, L. Cheng, Z. Zhang, J. Zhao, R. Bai, Z. Guo, W. Yu, X. Yan, *Nat. Commun.* **2022**, *13*, 6654; b) J. Zhao, Z. Zhang, L. Cheng, R. Bai, D. Zhao, Y. Wang, W. Yu, X. Yan, *J. Am. Chem. Soc.* **2022**, *144*, 872–882; c) J. Zhao, M. Hong, Z. Ju, X. Yan, Y. Cai, Z. Liang, *Angew. Chem. Int. Ed.* **2022**, *61*, e202214386; d) J. Deng, R. Bai, J. Zhao, G. Liu, Z. Zhang, W. You, W. Yu, X. Yan, *Angew. Chem. Int. Ed.* **2023**, *62*, e202309058.

[15] a) Y. Hou, Y. Peng, P. Li, Q. Wu, J. Zhang, W. Li, G. Zhou, J. Wu, *ACS Appl. Mater. Interfaces* **2022**, *14*, 35097–35104; b) B. Qiao, X. Zhao, D. Yue, L. Zhang, S. Wu, *J. Mater. Chem.* **2012**, *22*, 12339–12348; c) Y. Qiu, L. Wu, S. Liu, W. Yu, *ACS Appl. Mater. Interfaces* **2023**, *15*, 10053–10063.

[16] a) J. Zhang, C. Huang, Y. Zhu, G. Huang, J. Wu, *Polymer* **2021**, *231*, 124114; b) C. Tian, H. Feng, Y. Qiu, G. Zhang, T. Tan, L. Zhang, *Polym. Chem.* **2022**, *13*, 5368–5379; c) Z. Zhao, S. Chen, P. Zhao, W. Luo, J. Zuo, C. Li, *Angew. Chem. Int. Ed.* **2024**, e202400758.

[17] a) H. H. Winter, F. Chambon, *J. Rheol.* **1986**, *30*, 367–382; b) F. Chambon, Z. S. Petrovic, W. J. MacKnight, H. H. Winter, *Macromolecules* **1986**, *19*, 2146–2149.

[18] L. Cheng, X. Zhao, J. Zhao, S. Liu, W. Yu, *Macromolecules* **2022**, *55*, 6598–6608.

[19] a) S. V. Wanasisnghe, O. J. Dodo, D. Konkolewicz, *Angew. Chem. Int. Ed.* **2022**, *61*, e202206938; b) Z. Zhang, M. Rong, M. Zhang, *Prog. Polym. Sci.* **2018**, *80*, 39–93; c) O. R. Cromwell, J. Chung, Z. Guan, *J. Am. Chem. Soc.* **2015**, *137*, 6492–6495; d) N. Ballard, S. A. F. Bon, *Polym. Chem.* **2014**, *5*, 6789–6796; e) J. Harron, R. A. McClelland, C. Thankachan, T. T. Tidwell, *J. Org. Chem.* **1981**, *46*, 903–910; f) C. P. Nair, G. Clouet, P. Chaumont, *J. Polym. Sci. Part A: Polym. Chem.* **1989**, *27*, 1795–1809; g) Y. Amamoto, H. Otsuka, A. Takahara, K. Matyjaszewski, *Adv. Mater.* **2012**, *24*, 3975–3980.

[20] a) L. Cheng, S. Liu, W. Yu, *Polymer* **2021**, *222*, 123662; b) J. J. Lessard, L. F. Garcia, C. P. Easterlin, M. B. Sims, K. C. Bentz, S. Arencibia, D. A. Savin, B. S. Sumerlin, *Macromolecules* **2019**, *52*, 2105–2111; c) L. Cheng, B. Li, S. Liu, W. Yu, *Polymer* **2021**, *232*, 124159; d) W. Denissen, G. Rivero, R. Nicolaÿ, L. Leibler, J. M. Winne, F. E. Du Prez, *Adv. Funct. Mater.* **2015**, *25*, 2451–2457.

[21] M. Röttger, T. Domenech, R. van der Weegen, A. Breuillac, R. Nicolaÿ, L. Leibler, *Science* **2017**, *356*, 62–65.

[22] E. M. James, *Physical properties of polymers handbook*. Springer, New York, **2007**.

[23] a) W. F. M. Daniel, B. Joanna, M. Vatankhah-Varnoosfaderani, K. Matyjaszewski, J. Paturej, M. Rubinstein, A. V. Dobrynin, S. S. Sheiko. *Nat. Mater.* **2016**,*15*, 183–189; b) J. L. Self, C. S. Sample, A. E. Levi, K. Li, R. Xie, J. R. de Alaniz, C. M. Bates. *J. Am. Chem. Soc.* **2020**, *142*, 7567–7573; c) S. S. Sheiko, A. V. Dobrynin, *Macromolecules* **2019**, *52*, 7531–7546. d) M. Abbasi, L. Faust, M. Wilhelm. *Adv. Mater.* **2019**, *31*, 1806484; e) S. J. Dalsin, M. A. Hillmyer, F. S. Bates. *Macromolecules* **2015**, *48*, 4680−4691.

[24] a) H. M. Wyss, K. Miyazaki, J. Mattsson, Z. Hu, D. R. Reichman, D. A. Weitz, *Phys. Rev. Lett.* **2007**, *98*, 238303; b) K. Liu, L. Cheng, N. Zhang, H. Pan, X. Fan, G. Li, Z. Zhang, D. Zhao, J. Zhao, X. Yang, Y. Wang, R. Bai, Y. Liu, Z. Liu, S. Wang, X. Gong, Z. Bao, G. Gu, W. Yu, X. Yan, *J. Am. Chem. Soc.* **2021**, *143*, 1162–1170.

10.1002/anie.202406937

WILEY VCH

RESEARCH ARTICLE

Entry for the Table of Contents

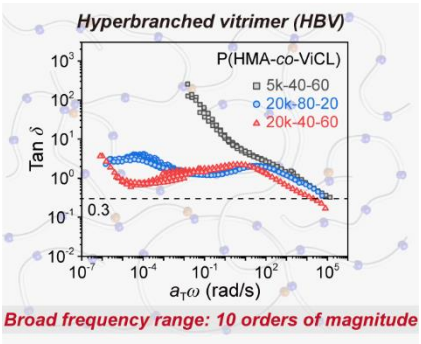

Polymers have been utilized as damping materials due to the high internal friction of molecular chains, enabling effectively dissipate energy as heat during service. Our work firstly presents hyperbranched vitrimers (HBVs) containing dense pendant chains and loose dynamic crosslinked networks, which exhibit ultrahigh energy-dissipation performance over a broad frequency range of nearly 10 orders of magnitude. This innovative design concept will provide opportunities for the further development of damping materials with multiple synergistic effects.